Traitement du Signal
Vol. 43, No. 3, June, 2026, pp. 1383-1393
Journal homepage: http://iieta.org/journals/ts

A Layered Multi-Channel Bluetooth Mesh Data Collection Protocol for Reliable and Energy-Efficient Transmission

Hongbo Yu*, Youpeng Wang, Haoyu Song, Jiadi Wei

School of Communication and Electronic Engineering, Qiqihar University, Qiqihar 161006, China

Corresponding Author Email: xgk029yhb@126.com

https://doi.org/10.18280/ts.430323

Received: 13 April 2026
Revised: 8 June 2026
Accepted: 20 June 2026
Available online: 30 June 2026

Keywords:
Bluetooth Mesh, layered multi-channel, hybrid acknowledgment mechanism, data collection

ABSTRACT

Conventional Bluetooth Low Energy (BLE) Mesh protocols employ a controlled flooding communication strategy, which inherently induces channel congestion. To address this issue, a layered multi-channel data collection protocol integrated with a hybrid acknowledgment policy was proposed. The conventional unconstrained flooding paradigm was abandoned, and a systematic optimization was achieved through a layered channel architecture. At the physical layer, a hop-count-based modulo-three channel allocation scheme was introduced, isolating the three advertising channels of the conventional BLE Mesh protocol in a spatially layered manner, thereby eliminating the channel contention environment caused by flooding. At the network layer, a directional routing strategy based on received signal strength indication was established for optimal parent node selection, replacing blind flooding with directed unicast transmission. At the data link layer, a node-level hybrid implicit-explicit acknowledgment policy was designed, which was driven by an exponentially weighted moving average adaptive window. This mechanism can effectively overcome timeout misjudgments induced by network congestion, guarantee high-reliability delivery, and simultaneously achieve link acknowledgment with zero extra overhead. Simulation results demonstrated that, under large-scale multi-hop networks and Monte Carlo random topological distributions, the proposed protocol significantly outperformed the conventional BLE Mesh flooding protocol in terms of robustness against high-concurrency interference. Substantial improvements were observed in end-to-end data delivery ratio, while overall network energy consumption was notably reduced, thereby extending the lifetime of the entire wireless sensor network. Notably, in small-to-medium-scale deployments (with network extents below 2000 m), the protocol drastically reduced multi-hop end-to-end latency. Under extremely large scales and high-concurrent loads, a trade-off was incurred, where increased transmission delay due to single-channel operation was exchanged for superior reliability performance.

1. INTRODUCTION

With the deep integration of Internet of Things technologies into domains such as indoor localization [1, 2], home automation [3, 4], smart agriculture [5, 6], and smart healthcare [7, 8], the deployment of large-scale, low-power wireless sensor networks has become a core infrastructure for achieving comprehensive environmental perception and device interconnectivity [9-11]. In these complex application scenarios, systems are frequently required to continuously collect substantial volumes of data from numerous nodes under high-concurrency conditions. Consequently, stringent demands are imposed on packet delivery ratio, age of information, and node-level energy consumption control. However, the existing conventional Bluetooth Mesh protocol primarily employs a controlled flooding mechanism at the network layer for data forwarding [12]. Under this paradigm, upon receiving a data packet, a node blindly rebroadcasts it to all neighboring nodes, relying mainly on message caching and time-to-live mechanisms. In typical many-to-one data collection scenarios, such as those found in smart agriculture, this unordered and concurrent flooding readily induces severe broadcast storms. When a large number of nodes attempt to access the channel simultaneously, the limited number of physical-layer primary advertising channels—namely, channels 37, 38, and 39—becomes rapidly congested within a short time, drastically reducing channel utilization [12-15].

Moreover, the conventional Bluetooth Mesh protocol lacks an efficient acknowledgment mechanism at the data link layer. To compensate for this deficiency in underlying reliability, the protocol often resorts to multiple blind retransmissions initiated at the application or network layer [16]. This strategy proves particularly detrimental at the "funnel neck" of a convergecast network, where all upstream sensor data streams are highly concentrated. The excessive redundant retransmission packets not only further increase end-to-end communication latency and exacerbate hidden-terminal and exposed-terminal collisions but also incur substantial and unnecessary energy dissipation [17-19]. For low-power embedded sensor nodes constrained by miniature battery supplies, the energy overhead arising from channel contention and blind retransmission irreversibly shortens the operational lifetime of hardware devices and may even lead to premature network topology partitioning. Therefore, in the face of large-scale, high-concurrency wireless data acquisition requirements, how to break free from the constraints of conventional limited-channel flooding, and to explore more efficient multi-channel coordinated scheduling and hybrid acknowledgment mechanisms—thereby reducing network power consumption while enhancing data delivery reliability—has become a critical challenge that urgently needs to be addressed in the field of low-power wireless communications.

At present, Bluetooth has been widely adopted in various agricultural domains. The potential of Bluetooth Low Energy (BLE) in smart agricultural unmanned aerial vehicle systems was analyzed by Maddikunta et al. [20], and an unmanned aerial vehicle control scheme was proposed in which smartphones and Bluetooth agricultural sensors were utilized as substitutes for conventional technologies such as Wi-Fi and ZigBee. A novel smart composting reactor prototype integrated with Bluetooth technology was designed and evaluated by Guidoni et al. [21]. In that system, remote and convenient monitoring of composting temperature was enabled through Bluetooth and a mobile application. In addition to significantly improving the final nitrogen concentration and seed germination rate, a 46.6% reduction in footprint was also achieved, thereby demonstrating the important value of Internet of Things technologies such as Bluetooth in the intelligent monitoring and performance enhancement of miniaturized agricultural and environmental protection equipment. A BLE-based smart soil probe system for spatiotemporal soil moisture mapping in precision agriculture was designed by Craven et al. [22]. In that study, BLE sensor nodes were deployed on the soil surface, and data were collected via a high-gain antenna mounted on a central pivot irrigation machine. During practical field deployment tests over a 50-hectare area, an effective Bluetooth packet transmission range of approximately 600 meters was achieved, and high-spatial-density spatiotemporal moisture maps of the field were successfully constructed. An Internet of Things- and Bluetooth-based intelligent lawn-mowing robot system was proposed by Aditya et al. [23], with the aim of addressing the low efficiency and high physical labor demands of traditional manual mowing. In that system, a microcontroller was employed as the core component, integrated with an HC-05 Bluetooth communication module and a real-time camera module, thereby enabling remote visual control of the device by operators through a smartphone application. A remote-controlled battery-powered rice direct seeder based on microcontroller and BLE technology was proposed by Komatineni et al. [24], intended to overcome the high labor intensity and operational difficulties associated with traditional manual seeding. Through that system, remote control of the seeder was made possible for operators from a safe and comfortable environment outside the field, using a Bluetooth application on a smartphone.

To address channel contention and resource allocation problems, various optimization schemes have been proposed in existing studies. A BLE-based monitoring gateway system for aquaculture environments was designed by Du et al. [25]. In that study, a queue mechanism and buffer management method were introduced to prioritize the delivery of critical information, and a feedback mechanism was employed to dynamically adjust node sampling periods according to the degree of parameter anomalies. Experimental results demonstrated that abnormal data were handled in a more timely and effective manner, with an average packet loss rate as low as 1.09%, and the transmission latency of critical information was significantly reduced. A precision agriculture monitoring framework based on BLE was proposed by Gautam and Kumar [26], in which battery-powered relay nodes were introduced to replace conventional cluster head nodes, thereby alleviating the data forwarding burden on underlying sensor nodes and extending communication coverage. Through simulation of the BLE Mesh broadcasting mechanism, relay nodes in that study were enabled to adaptively learn packet arrival patterns and wake up for scanning only during expected reception windows. An optimization method termed "controlled flooding bed" was proposed by Khanmirza and Maroufi [27] to address the high energy consumption of conventional flooding protocols under concurrent transmission mechanisms. In that study, a distributed leader election process was employed to determine root nodes, and a spanning tree was constructed among nodes to establish parent-child hierarchical relationships, thereby effectively preventing blind flooding of data into network regions where no demand existed. Through simulations and real-world validation on a small-scale testbed based on Bluetooth 5.0, the controlled flooding mechanism was shown to significantly reduce redundant concurrent transmissions while preserving the low-latency and high-reliability advantages of flooding networks, achieving up to 50% reduction in overall network energy consumption. This line of work provides an important reference for optimizing the underlying routing and distribution mechanisms of low-power Bluetooth networks.

To address the aforementioned challenges, a Bluetooth Mesh data collection protocol based on a layered multi-channel mechanism and a hybrid acknowledgment strategy is proposed in this work. First, at the physical layer, a hop-count-based modulo-three channel allocation and isolation mechanism is introduced. By leveraging the three advertising channels defined in the BLE protocol, nodes at adjacent hierarchical levels are assigned to different channels, thereby avoiding channel contention during simultaneous transmissions between nodes at neighboring levels and substantially accelerating transmission speed. Second, for nodes at the same hierarchical level, a directional routing strategy based on received signal strength indication for optimal parent node selection is employed, which effectively prevents the excessive channel and resource occupation caused by conventional node flooding propagation. Finally, at the data link layer, a node-level hybrid acknowledgment mechanism is proposed. This mechanism guarantees highly reliable data link delivery while utilizing the inherent data transmission from child nodes to parent nodes to accomplish the acknowledgment confirmation, thereby effectively alleviating congestion pressure at convergecast nodes and significantly reducing communication energy consumption across all network nodes.

2. SYSTEM MODEL

To rigorously articulate the design principles of the proposed improved Bluetooth Mesh networking protocol, a formalized modeling of the wireless multi-hop sensor network under investigation is first conducted in this section, and the limitations of the conventional Bluetooth Mesh flooding mechanism are quantitatively analyzed from a mathematical perspective. A wireless sensor network oriented toward large-scale environmental monitoring is considered herein. The multi-hop wireless sensor network is abstracted as a directed graph $G = (V, E)$, where $V = \{v_0, v_1, \ldots, v_n\}$ denotes the set of nodes in the network, v_0 represents the central gateway, and $v_i (i \in [1, n])$ represents the distributed sensor nodes. A directed edge $e_{i,j}$ in the edge set E indicates that node v_i is capable of successfully transmitting data to node v_j in a single hop.

All nodes in the network are assumed to be equipped with MS-BLE050R hardware radio frequency communication modules compliant with the BLE standard, and data transmission and reception are uniformly performed at the physical layer using the three orthogonal advertising channels (CH37, CH38, and CH39) specified by the BLE protocol. The constant transmission power of all network nodes is defined as P_{tx}, and the baseband sensitivity threshold for successful receiver demodulation is denoted as P_{th}. To account for the severe multipath effects and signal occlusion fading prevalent in complex monitoring environments such as agricultural greenhouses or dense vegetation areas, the log-distance path loss model is introduced to accurately characterize the large-scale fading characteristics of wireless signals. The path loss $PL(d_{i,j})$ of the link between a transmitting node v_i and a receiving node v_j [28] is calculated as shown in Eq. (1):

$$PL(d_{i,j}) = PL(d_0) + 10n\log_{10}\left(\frac{d_{i,j}}{d_0}\right) + X_\sigma \tag{1}$$

where, $d_{i,j}$ denotes the Euclidean physical distance between the transmitting node v_i and the receiving node v_j; d_0 is the far-field reference distance (typically set to 1 m); $PL(d_0)$ is the reference path loss at the corresponding reference distance; n is the path loss exponent, which reflects the spatial attenuation gradient in a specific complex environment; and $X_\sigma \sim \mathcal{N}(0, \sigma^2)$ is a Gaussian random variable with zero mean and standard deviation σ, employed to quantify the stochastic channel fluctuations induced by multipath and shadow fading effects. In large-scale concurrent transmission scenarios, channel contention becomes particularly severe. Whether a receiving node v_j can successfully decode a target data packet is essentially determined by whether the signal-to-interference-plus-noise ratio [29] at its physical-layer receiver reaches or exceeds the predefined demodulation threshold γ. The physical-layer anti-interference criterion is expressed as shown in Eq. (2):

$$SINR = \frac{P_{rx}(i,j)}{P_N + \sum_{k \in \mathcal{I}} P_{rx}(k,j)} \geq \gamma \tag{2}$$

where, $P_{rx}(i,j)$ denotes the effective signal power captured by the receiving node v_j from the target source node v_i; P_N is the ambient thermal noise power; the set $\mathcal{I}$ represents the aggregate set of other interfering nodes that are concurrently transmitting on the same physical channel within the same time window; and the denominator term $\sum_{k \in \mathcal{I}} P_{rx}(k,j)$ macroscopically represents the total co-channel interference power sustained at the receiver. The rapid increase of this term constitutes the mathematical essence of why the standard flooding mechanism is highly susceptible to inducing "broadcast storms" and physical-layer collisions in large-scale networks.

A refined energy consumption model is established herein for tree-topology Bluetooth Mesh nodes in low-power data acquisition scenarios. The core operating states of a node are categorized into only three types: transmitting, receiving, and idle. No independent "listening," "forwarding," or "backoff" states are defined. In this model, the channel listening performed during the implicit acknowledgment phase, as well as the clear channel assessment and backoff procedures of the medium access control layer carrier sense multiple access with collision avoidance mechanism, are both subsumed under the receiving state. The data forwarding process is accomplished through the sequential concatenation of the receiving state and the transmitting state. Since the switching time of the radio frequency module between different states is on the order of microseconds, the total energy consumption contributed by state transitions accounts for less than 0.1% of the overall energy budget; therefore, it is reasonably neglected in the model.

3. PROTOCOL DESIGN AND MECHANISM IMPLEMENTATION

In this section, the algorithmic principles, mechanism models, and overall communication procedures of the layered channel isolation module and the hybrid acknowledgment mechanism at the data link layer are elaborated in detail.

3.1 Layered channel isolation mechanism

To effectively eliminate the broadcast storms and co-channel collisions induced by the conventional Bluetooth Mesh flooding mechanism, a hop-count-based modulo-three channel allocation mechanism is proposed, utilizing the three native advertising channels (CH37, CH38, and CH39) defined by the BLE protocol, as illustrated in Figure 1. Based on the network model $\mathcal{G} = (\mathcal{V}, \mathcal{E})$ established in Section 1, this mechanism transforms the unordered blind flooding across the entire network into a spatially orthogonal, ordered pipeline transmission.

During the network initialization phase, an initial beacon frame with a hop-count field set to 0 is broadcast by the gateway node v_0 to its surrounding neighbors. After receiving the beacon, sensor node v_i selects its optimal parent node v_{parent} based on the received signal strength indication. The function $Hop(v_i)$ is defined as the minimum hop count from node v_i to the gateway v_0. For any node v_i, its hierarchical level H_i (i.e., $Hop(v_i)$) is calculated, as shown in Eq. (3):

$$H_i = H_{parent} + 1 \tag{3}$$

where, H_{parent} denotes the hierarchical level of the parent node selected. Through the above computational process and the flooding of beacons, the entire network is partitioned into a set of mutually disjoint logical subsets $\mathcal{L}_k = \{v_i \in V \mid H(v_i) = k\}$, and a tree-topology network structure rooted at the gateway v_0 is established, which guides data flows toward the gateway.

To achieve signal isolation between adjacent hierarchical layers, the protocol employs a modulo-three arithmetic rule to assign a fixed transmitting channel and a fixed receiving channel to each network layer. For any node v_i, its transmitting channel $CH_{TX}(i)$ and receiving channel $CH_{RX}(i)$ are respectively defined as shown in Eqs. (4) and (5):

$$CH_{TX}(i) = 37 + (H_i \% 3) \quad (4)$$

$$CH_{RX}(i) = 37 + ((H_i + 1)\% 3) \quad (5)$$

This allocation strategy ensures that the transmitting channel of sensor nodes at layer H_i is matched with the receiving channel of sensor nodes at layer $H_i - 1$, thereby forming a tree-shaped upstream data channel along the physical links. Furthermore, a spatial-reuse transmission strategy is realized by this mechanism: although layer H_i and layer $H_i + 3$ reuse the same physical channel, their physical separation is typically much larger than the signal interference radius; therefore, simultaneous data transmissions can be conducted without mutual interference. Layers H_i, $H_i + 1$, and $H_i + 2$ operate on three distinct channels, enabling parallel data transmission as well. By assigning different communication channels to sensor nodes, the extensive channel contention and the communication delays caused by random backoff in flooding propagation are avoided, thereby substantially raising the upper bound of network capacity.

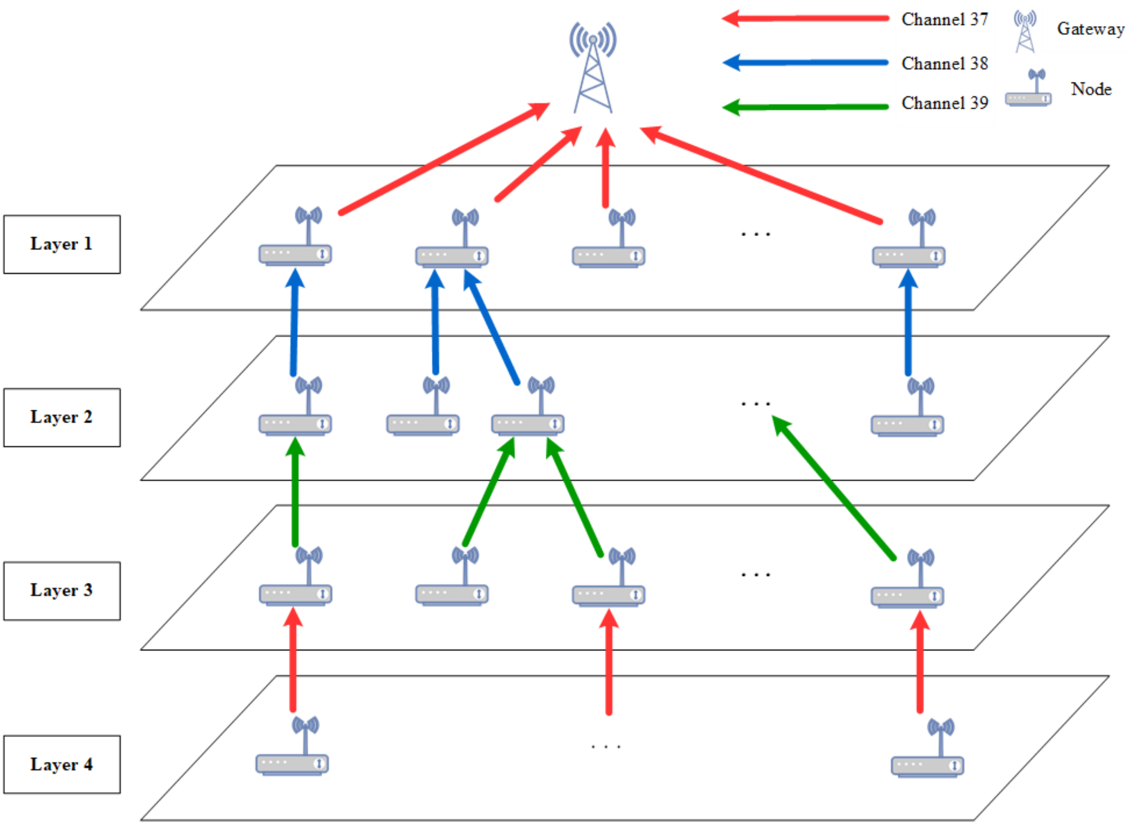

Figure 1. Schematic diagram of hop-count-based modulo-three layered channel allocation

Table 1. Custom application-layer communication frame

Field Name	Length (Bytes)	Description	Function
Frame type	1	Frame type identifier	Distinguishes data frame (0x01), explicit acknowledgment (0x02), and beacon (0x03)
Sequence number	1	Sequence number	Allows the child node to determine successful delivery by matching this field in forwarded frames
Source identifier	2	Source node identifier	Identifies the initial sender of the data packet
Destination identifier	2	Next-hop/destination identifier	Identifies the receiver of the data packet
Payload	N	Sensor data	Environmental data such as temperature, humidity, and illumination

It should be noted, however, that this channel allocation mechanism primarily eliminates inter-layer channel contention in the spatial domain. For collisions that may still occur when multiple child nodes within the same layer concurrently transmit to their parent node, the protocol addresses the contention problem by leveraging the native carrier sense multiple access with collision avoidance mechanism of the standard BLE medium access control layer, with a random backoff time window introduced to resolve same-layer concurrent transmission collisions.

3.2 Hybrid acknowledgment and retransmission mechanism

Although the layered channel mechanism can effectively eliminate collisions caused by channel contention, various factors in the wireless communication environment may still lead to packet loss. In the conventional Bluetooth Mesh networking scheme, packet loss is mitigated by simultaneously transmitting identical content over three channels. However, this blind transmission strategy incurs excessive overhead and lacks precise link-layer feedback on transmission status. To address this, a node-level hybrid acknowledgment mechanism is designed in this work. By leveraging the inherent broadcast nature of nodes, separate transmission of acknowledgment frames occupying channel resources is rendered unnecessary; thus, highly reliable data delivery over multi-hop networks is ensured with extremely low control overhead. To support the hybrid acknowledgment mechanism and enable reliable data traceability, a custom application-layer frame structure is designed atop the standard BLE link layer, as shown in Table 1. The data frame includes a frame control field, a sequence number, source/destination addresses, and a payload.

For the majority of relay forwarding nodes (H_i, with $H_i > 1$) in the entire network, an implicit acknowledgment scheme is employed. By leveraging the inherent broadcast nature of Bluetooth signals, after node H_i completes data transmission to its parent node $H_i - 1$, the radio frequency module is immediately switched to the receiving channel (i.e., the transmitting channel $CH_{TX}(parent)$ of the parent node $H_i - 1$) and a waiting time window T_{impl} is entered. If a data frame forwarded by the parent node $H_i - 1$ is overheard within this waiting time window, the source identifier and sequence number are extracted from the packet. If both fields exactly match those of the data packet just transmitted by the node itself, the parent node is determined to have successfully received the data. This mechanism cleverly utilizes the data forwarding process itself as an acknowledgment signal, thereby achieving link acknowledgment with zero overhead.

For the first-hop nodes (H_i, with $H_i = 1$) that are capable of communicating directly with the gateway, an explicit acknowledgment mechanism must be adopted, since their parent node (the gateway), as the data convergence endpoint, does not perform data forwarding. After data transmission, such nodes also switch to the parent node's transmitting channel and wait. In this case, the gateway is required to occupy the channel to transmit an acknowledgment frame; successful transmission is confirmed only when an acknowledgment frame from the gateway is received within the specified time window.

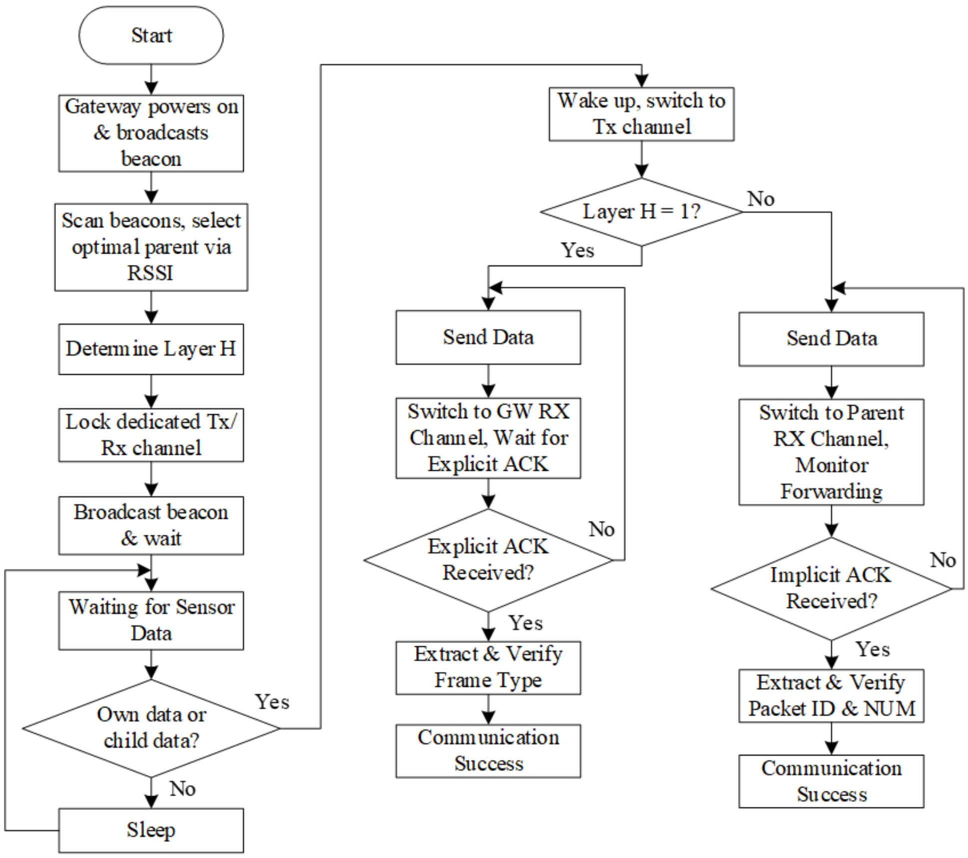

Figure 2. Overall networking communication flowchart of the node protocol

Note: RSSI = received signal strength indication; Tx/Rx = transmitting/receiving; Tx = transmitting; GW Rx = gateway receiving; ACK = acknowledgment; ID = identifier; NUM = number.

To address the forwarding latency incurred by parent nodes in practical networks due to medium access control layer's contention backoff, queue congestion, or processing delays, and to prevent child nodes from making erroneous judgments and unnecessary retransmissions caused by an overly short fixed waiting window, the static waiting window $implT$ is replaced in this work with an adaptive dynamically adjusted window $implT_k$. Relay nodes perform real-time estimation based on the exponentially weighted moving average of historical forwarding delays, with the update equation given in Eq. (6):

$$implT_k = \beta \cdot implT_{k-1} + (1-\beta) \cdot D_{actual} + D_{margin} \tag{6}$$

where, $implT_k$ denotes the implicit acknowledgment waiting window for the current data packet; $implT_{k-1}$ is the previous historical smoothed window value; D_{actual} is the actual time difference observed by the child node during the last successful overhearing of the parent node's forwarding; β is the smoothing factor (set to 0.4 in the experiments of this study); and D_{margin} is the tolerance margin, introduced to cover the random backoff delay induced by the carrier sense multiple access with collision avoidance mechanism of the standard BLE medium access control layer. If network load intensifies and queue congestion occurs at the parent node, an increase in D_{actual} automatically raises $implT_k$ for the next cycle, thereby enhancing the protocol's adaptive capability to dynamic high-concurrency load conditions.

3.3 Overall protocol communication procedure

As shown in Figure 2, the communication procedure of the proposed protocol is logically composed of two phases: network initialization and channel adaptation, and data communication with acknowledgment.

(i) Network Initialization and Channel Adaptation Phase

First, the gateway v_0 is powered on and enters the active broadcasting mode, periodically transmitting initial beacon frames with the hop-count field set to 0 (H = 0) in a round-robin manner over the three BLE channels. Sensor node v_i operate in a full-channel scanning state. Upon capturing a beacon, each node selects the node with the optimal and most stable signal quality as its parent node v_{parent}, and computes its own logical hierarchical level ($H_i = H_{parent} + 1$) based on the hop-count information of the parent node. During the process of acquiring potential parent node beacons, to cope with instantaneous received signal strength indication fluctuations induced by multipath effects and vegetation occlusion in complex wireless environments, an exponentially weighted moving average filtering algorithm is introduced in the node selection procedure. For node v_i, the update equation for the link quality estimate $RSSI_{smooth}$ of a potential parent node v_{parent} is given in Eq. (7):

$$RSSI_{smooth} = \alpha \cdot RSSI_{current} + (1-\alpha) \cdot RSSI_{last} \tag{7}$$

where, $RSSI_{smooth}$ denotes the smoothed link quality estimate obtained from the current calculation; $RSSI_{current}$ denotes the instantaneous received signal strength sampling value actually measured in the current cycle; $RSSI_{last}$ denotes the previously stored historical smoothed estimate; and α is the smoothing factor, which determines the weight of the instantaneous measurement in the overall estimate, and is set to 0.3 in this study. After the evaluation window period elapses, the node binds to the parent node with the optimal and most stable signal quality. Once the parent-child topological relationship is established, the sensor node computes and fixes its own transmitting channel CH_{TX} and corresponding receiving channel CH_{RX} using the modulo-three arithmetic rule, and continuously broadcasts its own beacon frames to surrounding nodes for capture by other sensor nodes. After all nodes complete channel adaptation, a layered tree-topology structure rooted at the gateway can be constructed across the entire network, and orthogonal channel isolation between hierarchical layers is accomplished at the physical level.

(ii) Same-Layer Directional Transmission Phase

When a sensor node needs to transmit its own sensor data, or when it acts as a relay node and receives a data packet to be forwarded from a child node, the data transmission procedure is triggered by the node. The internal state machine of the node is rapidly woken up, and a determination is made as to whether the data packet originates from one of its own child nodes. If not, the packet is directly discarded; if so, the node switches to transmission mode and transmits the packet to the optimal parent node, which has been selected based on received signal strength indication during the network initialization phase, on the fixed transmitting channel (CH_{TX}) locked. This directional transmission strategy avoids the broadcast storm caused by data flooding and improves channel utilization efficiency.

(iii) Hybrid Link Acknowledgment and Retransmission Phase

After data transmission is completed, the procedure immediately enters the hybrid link acknowledgment phase. The node dynamically executes the acknowledgment strategy according to its own hierarchical level H_i: for the first-hop nodes ($H_i = 1$) that communicate directly with the gateway, since the gateway, as the data sink, does not perform forwarding, the node is required to switch to the receiving channel and wait for a dedicated acknowledgment control frame from the gateway. For the relay forwarding nodes ($H_i > 1$), which constitute the majority of the network, the channel is adjusted to the parent node's transmitting channel, and a "zero-overhead" implicit acknowledgment is achieved by overhearing the parent node's forwarding behavior for that data frame. At this point, the listening window period of the relay node employs the adaptive window $implT_k$ described in Section 2.2. If a valid feedback is successfully overheard within the dynamic window, the node immediately updates the waiting window value for the next cycle based on the actual delay D_{actual} observed in this transmission and clears the retransmission counter. If the parent node's forwarding behavior is not overheard within the current $implT_k$, the link transmission is determined to have failed, and the node formally triggers the retransmission mechanism. This dynamic adjustment mechanism ensures both noise tolerance under high-load conditions and avoids energy waste caused by blind waiting under light-load conditions.

4. SIMULATION EXPERIMENTS AND RESULT ANALYSIS

To verify the performance of the proposed data collection protocol based on layered multi-channel and hybrid acknowledgment strategies, a comparative test environment was constructed using the ns-3 simulation platform. The conventional Bluetooth Mesh protocol was employed as the baseline control group, and the optimization effects of the proposed protocol were validated through multiple controlled-variable experiments. The simulation experiments were conducted from two dimensions: fundamental performance evaluation and robustness verification under complex environmental conditions.

4.1 Simulation environment setup

The ns-3 simulation tests were conducted on a computer equipped with an Intel Core i5-14600F central processing unit and 16.0 GB of random access memory, with an Ubuntu system installed in a VMware virtual machine. All experimental tests were performed under as consistent conditions as possible. The physical-layer parameters were configured strictly in accordance with the specifications of the MS-BLE050R hardware Bluetooth 5.0 module. Other specific simulation parameters are listed in Table 2.

4.2 Analysis of experimental results

Sensor nodes were distributed in a square grid pattern with a spacing of 200 meters, and the gateway node was deployed at the geometric center of the entire area. The number of sensor nodes (*N*) was calculated using Eq. (8):

$$N(L,d) = \left(\frac{L}{d}\right)^2 \quad (8)$$

where, L denotes the side length of the area, d denotes the fixed spacing of 200 meters, and $\frac{L}{d}+1$ represents the linear node density along the coordinate axes. The performance of the proposed protocol was compared with that of the conventional Bluetooth Mesh flooding protocol from three aspects: packet delivery ratio, average age of information, and total network energy consumption.

4.2.1 Packet delivery ratio simulation experiments

As shown in Figure 3, the variation trends of packet delivery ratio under different network scales are presented. It can be observed from the figure that, within the range of 400 m × 400 m, both protocols were able to maintain a packet delivery ratio of 100%. However, as the area expanded to 1600 m × 1600 m (with 64 nodes), the packet delivery ratio curve of the conventional Bluetooth Mesh protocol exhibited a significant downward trend, eventually dropping to 94%. This degradation is attributed to the fact that, with increasing hop counts, the channel contention induced by the flooding mechanism intensified sharply, resulting in substantial packet loss. In contrast, the improved Bluetooth Mesh protocol demonstrated superior performance, still achieving a packet delivery ratio close to 100%. Even under the largest-scale scenario, the delivery ratio remained at a high level, owing to the modulo-three channel isolation mechanism, the contention-free directional transmission strategy, and the retransmission guarantee provided by the hybrid acknowledgment mechanism.

4.2.2 Average age of information simulation experiments

As shown in the experimental results in Figure 4, before the area reached 2600 m × 2600 m, the improved Bluetooth Mesh protocol was able to maintain a consistently low age of information, indicating that newly generated sensor data could be delivered to the gateway more rapidly. This advantage is primarily attributed to the speed gains enabled by the layered channel allocation and directional transmission. However, it can be observed that beyond this point, the age of information increased substantially compared with that of the conventional Bluetooth Mesh protocol. Combined with the analysis of the overall flowchart in Figure 2, this phenomenon can be explained as follows: in the conventional Bluetooth Mesh protocol, data are transmitted over three channels without an acknowledgment mechanism, and blind flooding propagation ensures that successful delivery is considered achieved as long as any one of the three channels is received by the gateway. In contrast, the improved protocol employs single-channel communication. In communication links exceeding 14 hops, packet loss coupled with retransmission-induced latency leads to a noticeable increase in the average age of information. Nevertheless, as can be seen from Figure 3, the data delivery ratio remained high under these conditions, thereby ensuring data integrity.

Table 2. Simulation and test environment parameters

Parameter Category	Parameter Name	Parameter Value
Test environment	Virtual machine version	VMware® Workstation 17 Pro 17.6.4
	Linux version	Ubuntu 22.04
	Simulation tool	ns-3 (v3.38)
Test parameters	Packet interval	60 seconds
	Simulation time	600 seconds
	Node distribution	Grid distribution
	Theoretical communication distance	300 meters
	Path loss exponent	2.66
	Radio frequency transmission current (0 dBm)	VDD=3.3 V, 4.8 mA
	Radio frequency reception current	VDD=3.3 V, 5.3 mA
	Transmission power	10 dBm
	Reception sensitivity	-96 dBm
	Payload size	32 bytes

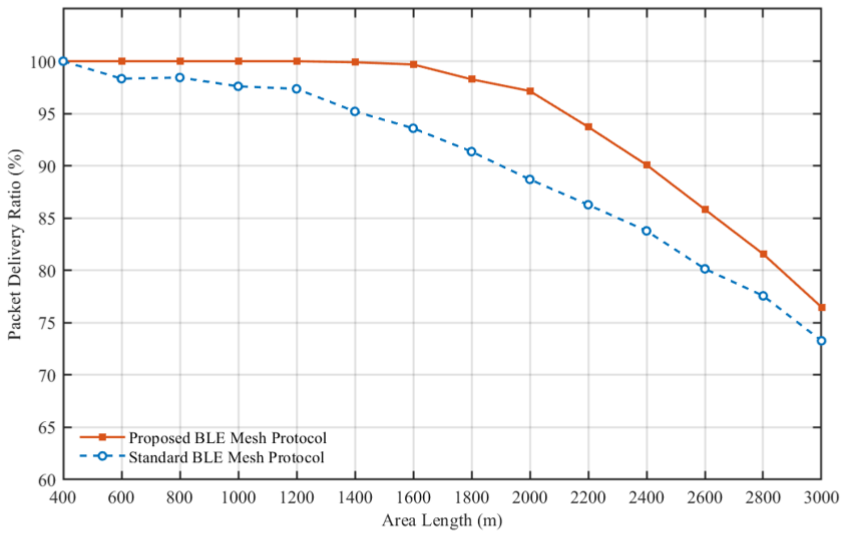

Figure 3. Comparison of packet delivery ratio between the two protocols under different network areas

4.2.3 Total network energy consumption simulation experiments

Figure 5 presents a comparison of the total network energy consumption of the two protocols under different scenarios. As can be observed from the figure, with the expansion of network scale, the energy consumption of the conventional Bluetooth Mesh protocol increased exponentially, reaching as high as 42,616 mJ in the 3000 m × 3000 m area. This is attributed to the fact that the flooding mechanism lacks routing guidance, resulting in a network flooded with a large number of redundant forwarding packets; moreover, the blind retransmissions caused by the absence of an acknowledgment mechanism further aggravate energy waste. In contrast, the improved Bluetooth Mesh protocol exhibited remarkably high energy efficiency, with a total energy consumption of only approximately 15,338 mJ, which is about 36% of that of the baseline protocol. This energy saving stems from two aspects: first, the directional routing based on received signal strength indication eliminates a large number of ineffective redundant broadcasts, thereby preventing blind forwarding of packets; second, the implicit acknowledgment mechanism enables relay nodes to complete acknowledgments without transmitting additional acknowledgment control frames, which significantly extends the operational time and lifetime of sensor nodes.

4.3 Robustness analysis under Monte Carlo random topologies

To overcome the limitations of regular grid topologies in evaluating network connectivity and to more objectively verify the robustness of the protocol under non-uniform node distribution scenarios, Monte Carlo method-based simulation experiments were conducted using uniform Poisson point process distributions. For each area gradient, 30 independent random node deployments were executed, and line charts of packet delivery ratio and the number of isolated nodes as functions of the area side length were plotted, as shown in Figure 6 and Figure 7, respectively.

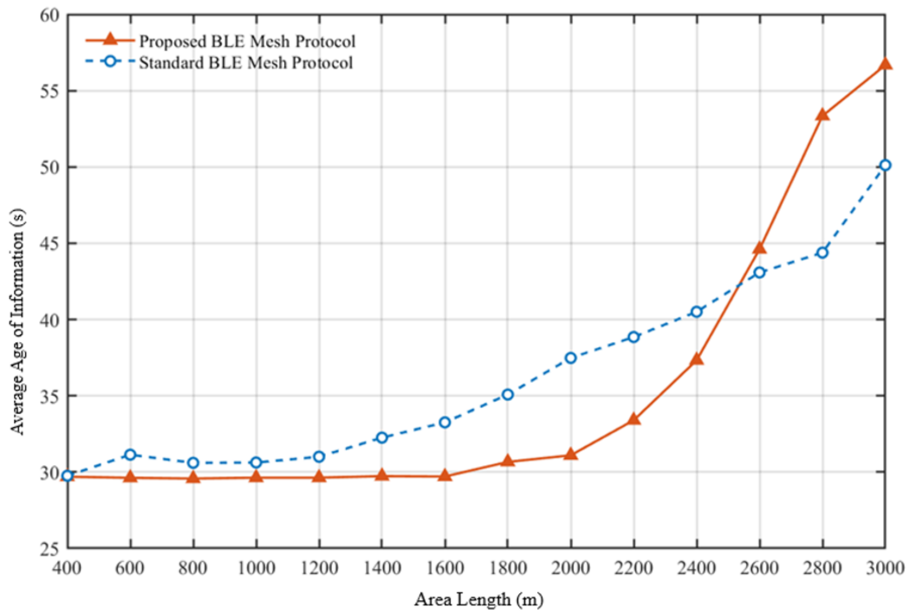

Figure 4. Comparison of average age of information between the two protocols under different network areas

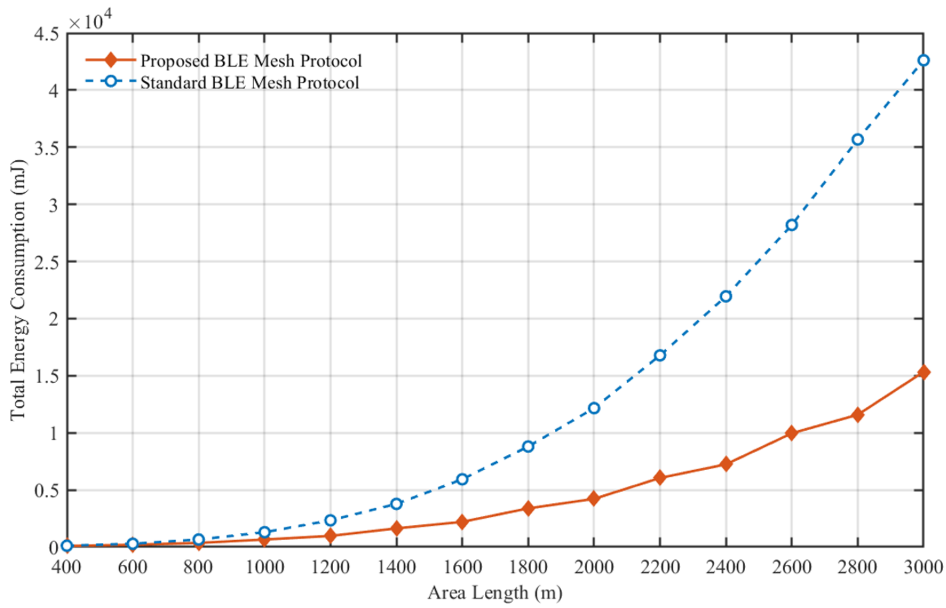

Figure 5. Comparison of total network energy consumption between the two protocols under different network areas

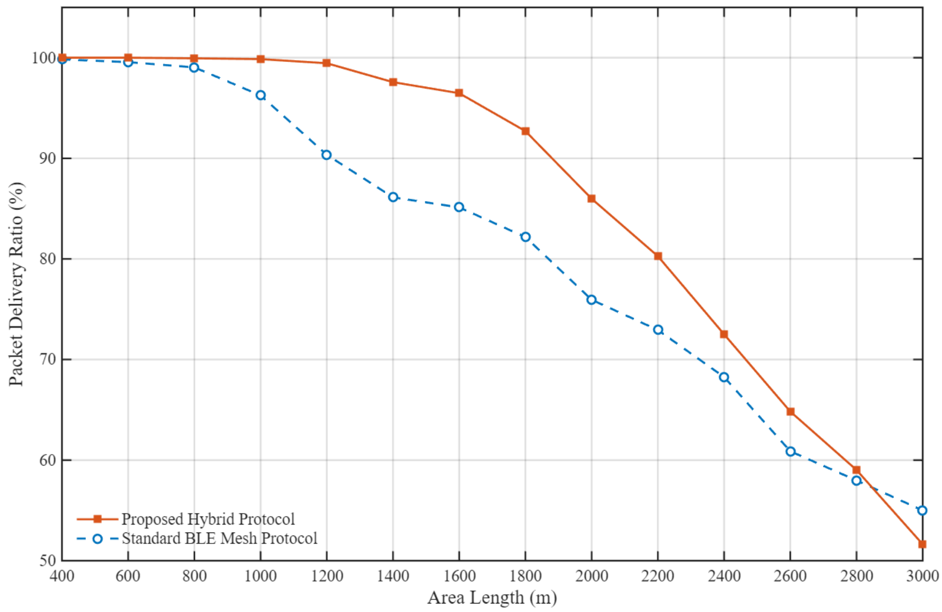

Figure 6. Comparison of packet delivery ratio between the two protocols under random topologies

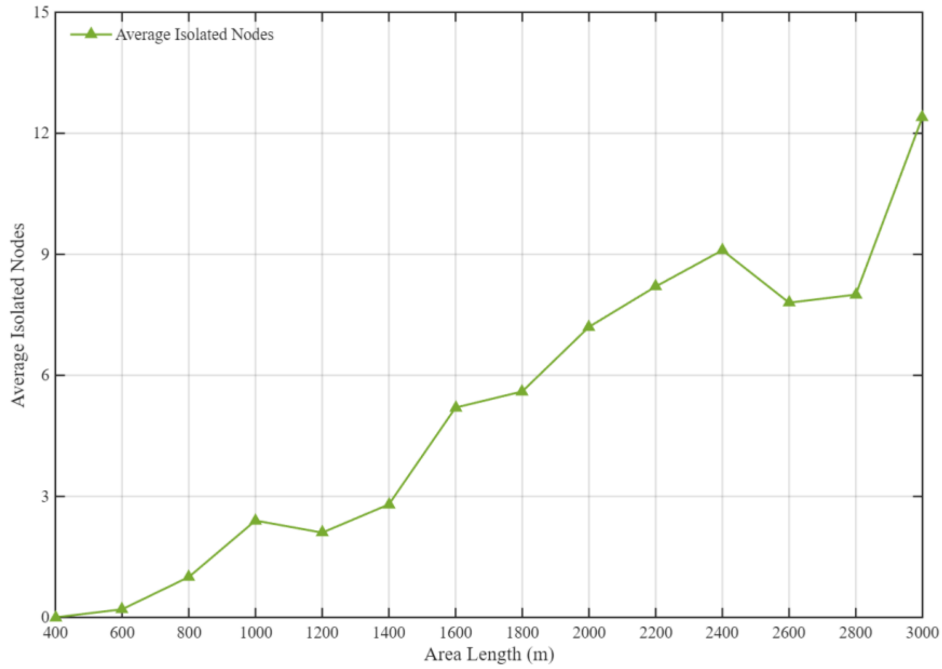

Figure 7. Number of isolated nodes under random topologies

Robustness analysis of the packet delivery ratio under high concurrency is described below. As can be observed from the curves in Figure 6, in small- to medium-scale scenarios with area side lengths below 1000 m × 1000 m, the proposed hybrid protocol consistently maintained the packet delivery ratio at an extremely high level exceeding 99.8%, whereas the packet delivery ratio of the conventional BLE Mesh protocol had already begun to exhibit a notable downward trend. This indicates that in regions with high local node density caused by random topologies, the blind flooding of the conventional protocol is highly prone to triggering severe "broadcast storms," resulting in substantial packet loss due to co-channel collisions. In contrast, the improved protocol, by virtue of the physical-layer modulo-three channel isolation and the network-layer directional unicast strategy, successfully avoided collisions induced by local node densification. As the area scale further expanded to medium-large scales (from 1200 m × 1200 m to 2000 m × 2000 m), the packet delivery ratio of the conventional protocol dropped to 75.94%. By comparison, the packet delivery ratio curve of the improved protocol declined more gently, still maintaining a level of 96.47% at 1600 m × 1600 m. This fully demonstrates that, under complex multi-hop link environments, the improved protocol exhibits excellent transmission robustness and system stability.

Figure 7 clearly illustrates the increasing trend in the average number of isolated nodes across the entire network as the area expands. When the area exceeded 2000 m × 2000 m, the average number of isolated nodes surpassed 7, and the proportion of isolated nodes remained persistently high, indicating that at such large geographical extents, the random uniform distribution led to severe local fragmentation and topological sparsity. Combined with the observations in Figure 6 for the extreme scales from 2600 m × 2600 m to 3000 m × 3000 m, it can be found that under edge scenarios where the network is extremely sparse and topological discontinuities occur, the packet delivery ratio of the improved protocol at 3000 m × 3000 m was 51.63%, slightly lower than the 55.00% of the conventional protocol. This is attributed to the fact that in such extreme scenarios with numerous isolated nodes and fragile single-link paths, the single-channel directional transmission of the improved protocol relies heavily on a single optimal parent node and lacks the fault-tolerance support of redundant paths. Once a critical relay node fails to establish a link due to random sparsity, the upstream channel is blocked. In contrast, the conventional protocol, by virtue of multi-channel omnidirectional blind flooding, has a slight probability of delivering data packets to the gateway through residual occasional paths.

Taken together, the simulation results from both figures indicate that, although the single-channel transmission encounters a fault-tolerance bottleneck in a very few edge scenarios of extreme sparsity, under the regular deployment densities and multi-hop scales typically required for practical agricultural environmental monitoring, the proposed protocol demonstrates superior comprehensive advantages in terms of data delivery reliability, anti-interference stability, and energy consumption control.

5. CONCLUSION

A Bluetooth Mesh protocol based on layered multi-channel and hybrid acknowledgment mechanisms was proposed in this work, addressing the issues of low delivery ratio and excessive power consumption caused by flooding propagation in conventional Bluetooth Mesh multi-hop networking. Through the modulo-three algorithm at the physical layer, hop-count-based layered channel isolation was realized, effectively avoiding co-channel interference. At the network layer, a directional routing strategy based on received signal strength indication was introduced, eliminating the broadcast storms induced by blind flooding. At the link layer, a hybrid implicit-explicit acknowledgment mechanism with an exponentially weighted moving average adaptive window was designed, effectively overcoming timeout misjudgments caused by parent node queue congestion and random backoff, while ensuring data transmission reliability with extremely low control overhead. Through optimization at these three layers, high stability was maintained even in large-scale networks, with substantially improved delivery ratio and reduced communication latency. Benefiting from the reduction in redundant broadcast transmissions and the optimization of the acknowledgment mechanism, total network energy consumption was reduced by approximately 64%, significantly extending the lifetime of the sensor network. Furthermore, Monte Carlo random topology experiments further confirmed that the protocol effectively avoids broadcast storms caused by the high-density clustering of local nodes, demonstrating excellent transmission stability. Although single-channel directional transmission encounters certain fault-tolerance path bottlenecks under edge scenarios of extreme sparsity and topological fragmentation, under regular deployment densities, the overall networking performance of the proposed scheme still exhibits superior comprehensive advantages. Future research may further explore improvements to the algorithm in reducing the average age of information. Overall, the protocol is more suitable for energy-sensitive Internet of Things applications with relatively fixed topologies, such as environmental monitoring, and provides support for promoting large-scale deployment of Internet of Things sensors.

REFERENCES

[1] Amoran, A.E., Oluwole, A.S., Fagorola, E.O., Diarah, R.S. (2021). Home automated system using Bluetooth and an android application. Scientific African, 11: e00711. https://doi.org/10.1016/j.sciaf.2021.e00711

[2] Szyc, K., Nikodem, M., Zdunek, M. (2023). Bluetooth low energy indoor localization for large industrial areas and limited infrastructure. Ad Hoc Networks, 139: 103024. https://doi.org/10.1016/j.adhoc.2022.103024

[3] Talla-Chumpitaz, R., Castillo-Cara, M., Orozco-Barbosa, L., García-Castro, R. (2023). A novel deep learning approach using blurring image techniques for Bluetooth-based indoor localisation. Information Fusion, 91: 173-186. https://doi.org/10.1016/j.inffus.2022.10.011

[4] Anitha, G., Sathya, M., Suganeswar, S., Vignesh Raja, G. (2021). Bluetooth based home automation and security system. Journal of Physics: Conference Series, 1916(1): 012106. https://doi.org/10.1088/1742-6596/1916/1/012106

[5] Nikodem, M. (2021). Bluetooth low energy livestock positioning for smart farming applications. In International Conference on Computational Science, Cham: Springer International Publishing, pp. 55-67. https://doi.org/10.1007/978-3-030-77970-2_5

[6] Sun, L., Sun, H., Cao, N., et al. (2022). Intelligent agriculture technology based on internet of things. Intelligent Automation and Soft Computing, 32(1): 429-439. https://doi.org/10.32604/iasc.2022.021526

[7] Tipparaju, V.V., Mallires, K.R., Wang, D., Tsow, F., Xian, X. (2021). Mitigation of data packet loss in bluetooth low energy-based wearable healthcare ecosystem. Biosensors, 11(10): 350. https://doi.org/10.3390/bios11100350

[8] Chang, C.S., Wu, T.H., Wu, Y.C., Han, C.C. (2023). Bluetooth-based healthcare information and medical resource management system. Sensors, 23(12): 5389. https://doi.org/10.3390/s23125389

[9] Choi, S.K., Kim, W.H., Sohn, I. (2023). Optimizing lifetime of Internet-of-Things networks with dynamic scanning. Mathematics, 11(23): 4768. https://doi.org/10.3390/math11234768

[10] Wang, T., Hou, D., Feng, L., Zhang, W., Rao, S. (2023). Temperature and humidity wireless sensor system based on Bluetooth low energy and solar self-power. Journal of Physics: Conference Series, IOP Publishing, 2615(1): 012014. https://doi.org/10.1088/1742-6596/2615/1/012014

[11] Nandal, V., Dahiya, S. (2023). A comprehensive review of energy efficient wireless communication and routing protocols in smart agriculture. International Journal of Sensor Networks, 43(2): 99-115. https://doi.org/10.1504/IJSNET.2023.134308

[12] Lin, B., Su, H. (2023). Experimental evaluation and performance improvement of bluetooth mesh network with broadcast storm. IEEE Access, 11: 137810-137820. https://doi.org/10.1109/ACCESS.2023.3339795

[13] Nahas, B.A., Escobar-Molero, A., Klaue, J., Duquennoy, S., Landsiedel, O. (2021). BlueFlood: Concurrent transmissions for multi-hop Bluetooth 5—Modeling and evaluation. ACM Transactions on Internet of Things, 2(4): 1-30. https://doi.org/10.1145/3462755

[14] Mohsin, S.K., Mohammed, M.A., Yassien, H.M. (2021). Developing of Bluetooth mesh flooding between source-destination linking of nodes in wireless sensor networks. Eastern-European Journal of Enterprise Technologies, 6(9): 6-14. https://doi.org/10.15587/1729-4061.2021.248978

[15] Wang, L., Li, J., Li, M. (2024). A rapid flooding approach based on adaptive delay and low-power sleep for BLE mesh networks. IEEE Access, 12: 65323-65332. https://doi.org/10.1109/ACCESS.2024.3398348

[16] Pierleoni, P., Gentili, A., Mercuri, M., Belli, A., Garello, R., Palma, L. (2021). Performance improvement on reception confirmation messages in Bluetooth mesh networks. IEEE Internet of Things Journal, 9(3): 2056-2070. https://doi.org/10.1109/JIOT.2021.3090656

[17] Gotz, J.D., Rayel, O.K., Moritz, G.L. (2021). Improving bluetooth mesh energy efficiency using clustering. Journal of Communication and Information Systems, 36(1): 156-165. https://doi.org/10.14209/jcis.2021.17

[18] Villa, D., Lin, C.K., Kuenzi, A., Lang, M. (2022). Bluetooth Low Energy mesh network for power-limited, robust and reliable IoT services. arXiv preprint arXiv:2208.04050. https://doi.org/10.48550/arXiv.2208.04050

[19] Hortelano, D., Olivares, T., Ruiz, M.C. (2021). Reducing the energy consumption of the friendship mechanism in Bluetooth mesh. Computer Networks, 195: 108172. https://doi.org/10.1016/j.comnet.2021.108172

[20] Maddikunta, P.K.R., Hakak, S., Alazab, M., et al. (2021). Unmanned aerial vehicles in smart agriculture: Applications, requirements, and challenges. IEEE Sensors Journal, 21(16): 17608-17619. https://doi.org/10.1109/JSEN.2021.3049471

[21] Guidoni, L.L.C., Corrêa, É.K., Moncks, P.C.S., et al. (2024). Innovation for recycling of organic matter through composter with automatic and sustainable temperature recording accessed via Bluetooth/mobile app. Environmental Monitoring and Assessment, 196(11): 1093. https://doi.org/10.1007/s10661-024-13285-8

[22] Craven, S., Bee, A., Sanders, B., et al. (2025). Smart Bluetooth stakes: Deployment of soil moisture sensors with rotating high-gain antenna receiver on center pivot irrigation boom in a commercial wheat field. Sensors, 25(17): 5537. https://doi.org/10.3390/s25175537

[23] Aditya, Y., Yasasri, B., Priya, A.J., Devi, D.N., Madhukar, E. (2024). Bluetooth controlled green sward cutter using IoT. In 2024 International Conference on Emerging Systems and Intelligent Computing (ESIC), Bhubaneswar, India, pp. 411-415. https://doi.org/10.1109/ESIC60604.2024.10481584

[24] Komatineni, B.K., Satpathy, S.K., Reddy, K.K.V., Sukdeva, B., Dwivedi, U., Lahre, J. (2023). Development and evaluation of bluetooth based remote controlled battery powered drum seeder. E-Prime-Advances in Electrical Engineering, Electronics and Energy, 6: 100333. https://doi.org/10.1016/j.prime.2023.100333

[25] Du, Y., Sun, G., Zheng, B., Qu, Y. (2021). Design and implementation of intelligent gateway system for monitoring livestock and poultry feeding environment based on bluetooth low energy. Information, 12(6): 218. https://doi.org/10.3390/info12060218

[26] Gautam, S., Kumar, S. (2024). Low-power BLE relay node operation in mesh-like architectures for precision agriculture. IEEE Sensors Journal, 24(20): 33347-33360. https://doi.org/10.1109/JSEN.2024.3451987

[27] Khanmirza, H., Maroufi, S. (2024). Good flood bed: An energy-efficient and controlled concurrent transmission protocol. International Journal of Wireless Information Networks, 31(2): 109-120. https://doi.org/10.1007/s10776-024-00618-0

[28] Liu, C., Zhang, Y., Zhou, H. (2021). A comprehensive study of bluetooth low energy. Journal of Physics: Conference Series, 2093(1): 012021. https://doi.org/10.1088/1742-6596/2093/1/012021

[29] Nagaraj, S. (2024). On mitigating the mismatch between FSK tags and GFSK receivers in BLE backscatter. IEEE Journal of Radio Frequency Identification, 9: 1-5. https://doi.org/10.1109/JRFID.2024.3514534